Comprehensive Journal of Science

مجلة العلوم الشاملة

Volume (10), Issue (37), (NOV. 2025)

عدد خاص بالمؤتمر الدولي الثالث للعلوم والتقنية

SICST2025, www.sicst.ly

المجلد (10)، العدد (37)، (نوفمبر2025)

ISSN: 3014-6266

ردمد: 3014-6266

A Comparative Analysis of Classical and Modern DTC Strategies for Induction Motor Drives via MATLAB/Simulink Simulation

Mohamed A. Mawma*1

Department of Electrical Engineering Technologies

Higher Institute of Engineering Technology Zliten- Libya (HIETZ)

www.mohmawma@gmail.com

Mahamud s Alwajawaj2

Department of Electrical Engineering Technologies

Higher Institute of Engineering Technology Zliten-Libya (HIETZ)

www.mhmwdalwjwaj6@gmail.com

Received: 30-09-2025; Revised: 10-10-2025; Accepted: 31-10-2025; Published: 25-11-2025

Abstract

Direct Torque Control DTC is a prominent high-performance control strategy for induction motor IM derives, prized for its rapid dynamic response and structural simplicity. However, classical DTC is plagued by inherent drawbacks, including significant torque and flux ripple, variable switching frequency, and high current total harmonic distortion THD. This paper presents a comprehensive comparative analysis of classical DTC against two modern variants: DTC with Space Vector Modulation (DTC-SVM) and Fuzzy Logic Control-based DTC (DTC-FLC). The performance evaluation is conducted through high-fidelity MATLAB/Simulink models under identical operating conditions. Key Performance Indicators KPIs such as torque ripple, flux ripple, stator current THD, and dynamic response are rigorously analyzed. The results demonstrate the superior performance of modern DTC techniques. DTC-FLC achieves a remarkable 87.5% reduction in torque ripple and stator current THD of only 2.18%, alongside improved transient performance by mitigating overshoot. DTC-SVM offers a robust alternative with a 70.9% torque ripple reduction and stator current THD of 4.12%, besides a fixed switching frequency. The study concludes with application-based recommendations, guiding the selection of the optimal DTC strategy for specific industrial needs

Keywords: Direct Torque Control (DTC); Induction Motors (IMs); Fuzzy Logic Control (FLC); Total Harmonic Distortion (THD).

Introduction

Induction motors (IMs) are the cornerstone of modern industrial systems due to their rugged construction, reliability, low cost, and minimal maintenance needs. Selecting

a suitable motor for a specific drive application is a complex process. Rajput et al. (2020) pointed out the associated parameters should be determined promptly and accurately from manufacturer's datasheet. Typically, the energy approach is designed using an equivalent motor circuit, with several variants proposed by Toliyat and Kliman (2018). Among these, the T-circuit configuration is considered as the most useful representation.

T- circuit configuration and its Equivalent Thevenin circuit simplification are depicted in figures 1, 2 respectively.

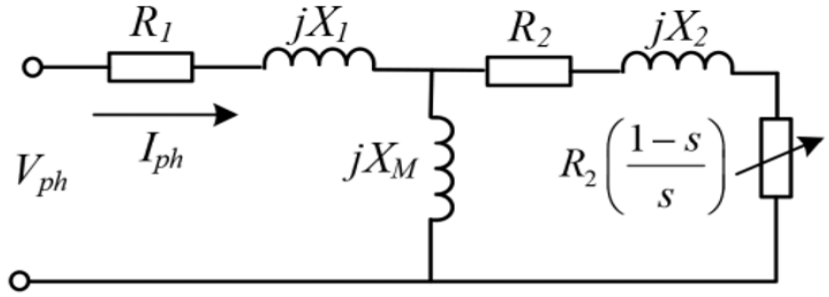

Figure 1: Equivalent T-circuit of 3-phase AC motor reduced to single phase.

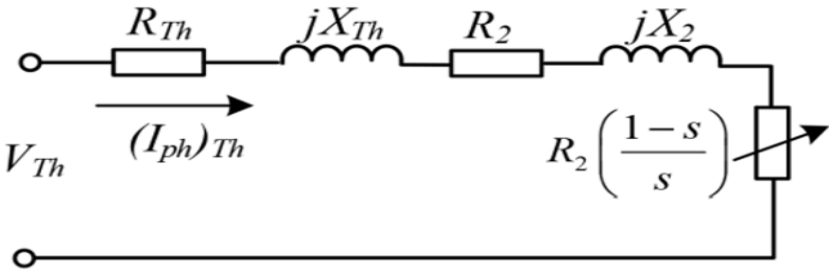

Figure 2: Equivalent Thevenin circuit simplification of AC motor.

The evolution of high performance control schemes for Induction Motors have been a central research focus in power electronics and drives. While field-oriented control (FOC) provides decoupled torque and flux control, its implementation complexity and sensitivity to machine parameters motivated the development of direct torque control DTC. Pioneered by Takahashi and T. Noguchi; Depenbrock (in the mid-1980s), classical DTC simplifies the control structure by directly regulating electromagnetic torque and stator flux linkage through the optimal selection of voltage vectors from an inverter. This hysteresis-based control strategy delivers unparalleled torque dynamics. Subsequent researches for instance those by P. Vas (1998); T. Noguchi (2002) assured that despite its advantages, the inherent hysteresis control introduces critical limitations: high torque and flux ripple, particularly at low speeds; variable switching frequency, complicating thermal and acoustic design; and high stator current THD, leading to increased losses and acoustic noise. In recent years, various advanced DTC strategies have been emerged to mitigate these issues, and address the limitations of conventional DTC. These methods rely on instantaneous torque and stator flux regulation, with inverter control signals directly derived from a switching table. Ouanjli et al. (2019) proposed that they are generally classified into two groups : conventional and advanced techniques. Examples include Space Vector Modulation (SVM), sliding mode-based DTC, model predictive DTC,

and artificial intelligence approaches such as fuzzy logic, neural networks, and genetic algorithms. The classification of strategies involved to improve the DTC control of an induction motor are illustrated in figure 3.

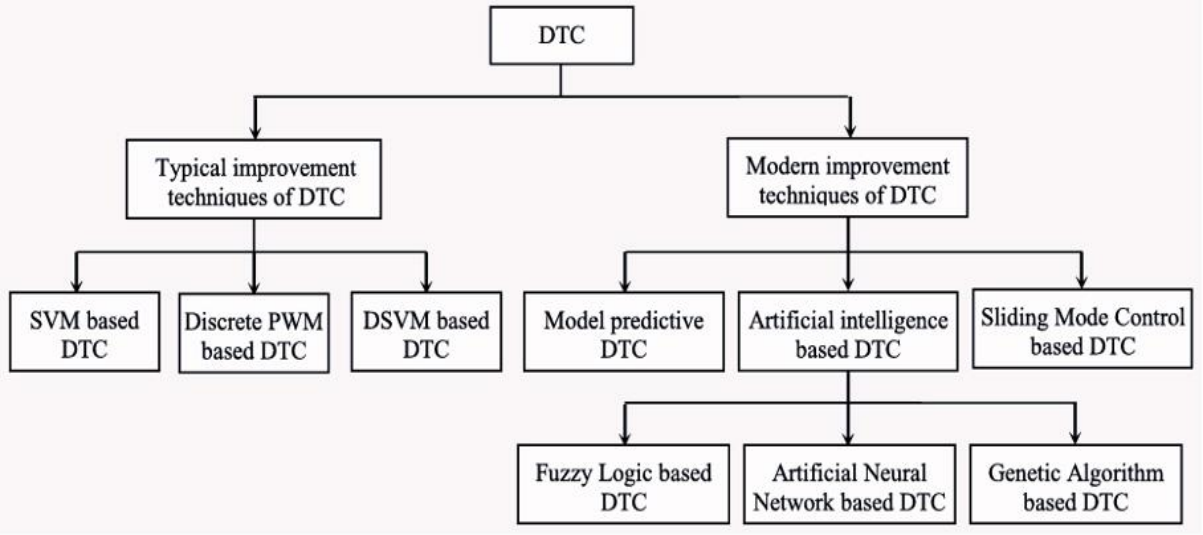

Figure 3: Classification of improvement techniques of Direct Torque Control

To mitigate the limitations of classical DTC such as ripple issues, Space Vector Modulation SVM has been incorporated into DTC frameworks. By enforcing a constant switching frequency, SVM reduces the harmonic distortion and improves voltage utilization. Studies such as those by F. Ben Salem et al. (2024) integrated an adaptive fractional-order sliding mode control process within DTC-SVM scheme, enhancing robustness and dynamic performance for electric vehicle propulsion systems. This combination leads to smoother torque and flux trajectories and improved response under transient conditions. Fuzzy Logic Controller FLC has been utilized to adaptively enhance DTC performance under varying operation conditions. The work of Korkmaz et al. (2013) demonstrated that FLC-based SVM can effectively attenuate high torque ripple by adjusting voltage vectors according to fuzzy rules. Additionally, combining FLC with current-limiting strategies further enhances the system's stability and mitigates performance degradation due to parameter uncertainties or load disturbances highlighted by Ortega et al. (2005). While numerous advanced DTC strategies, such as DTC-SVM and DTC-FLC, have been proposed to mitigate the well-known limitations of Classical DTC (high ripple, variable switching frequency), a definitive comparative analysis under unified operating conditions is absent. The lack of a standardized performance evaluation using key metrics like torque ripple, current THD, and dynamic response makes it difficult to quantify their relative advantages and provide clear selection guidelines for specific industrial applications. This research work investigates three DTC strategies for induction motors IM. The first is conventional DTC (C-DTC), where hysteresis controllers regulate torque and flux. The second is space vector modulation DTC (SVM-DTC), employing PI regulators. The third is fuzzy base-DTC, where fuzzy logic regulates torque and flux ripples.

Induction Motor Model

P. Vas (1998) described the dynamic model of a three-phase induction motor in the stationary reference frame (α-β) by the following equations :

- Stator Voltage Equations:

$$v_{s\alpha} = R_s i_{s\alpha} + \frac{d\,\psi_{s\alpha}}{dt} \quad (1)$$

$$v_{s\beta} = R_s i_{s\beta} + \frac{d\,\psi_{s\beta}}{dt} \quad (2)$$

- Rotor Voltage equations:

Since, the rotor bars of a squirrel-cage induction motor are shorted:

$$v_{r\alpha} = v_{r\beta} = 0$$

$$0 = R_r i_{r\alpha} + \frac{d\,\psi_{r\alpha}}{dt} + \omega_r \psi_r \beta \quad (3)$$

$$0 = R_r i_{r\beta} + \frac{d\,\psi_{r\beta}}{dt} - \omega_r \psi_r \alpha \quad (4)$$

- Stator and Rotor Flux Linkage Equations:

$$\psi_{s\alpha} = L_s i_{s\alpha} + L_m i_{r\alpha} \quad (5)$$

$$\psi_{s\beta} = L_s i_{s\beta} + L_m i_{r\beta} \quad (6)$$

$$\psi_{r\alpha} = L_m i_{s\alpha} + L_r i_{r\alpha} \quad (7)$$

$$\psi_{r\beta} = L_m i_{s\beta} + L_r i_{r\beta} \quad (8)$$

- Electromagnetic Torque:

$$T_e = \frac{3}{2} P\left(\psi_{s\alpha} i_{s\beta} - \psi_{s\beta} i_{s\alpha}\right) \quad (9)$$

Where, $v_{s\alpha}$, $v_{s\beta}$, $v_{r\alpha}$ and $v_{r\beta}$ represent the stator and the rotor voltages respectively in the stationary α -β reference frame, while $i_{s\alpha}$, $i_{s\beta}$, $i_{r\alpha}$ and $i_{r\beta}$ denote the corresponding stator and rotor currents respectively. The stator and rotor resistances are R_s , R_r . The stator and the rotor flux linkages are given by $\psi_{s\alpha}$, $\psi_{s\beta}$, $\psi_{r\alpha}$ and $\psi_{r\beta}$ .The rotor electrical angular velocity is ω_r. The inductances L_s , L_r and L_m correspond to the stator, rotor and magnetizing components respectively. The number of pole pairs is denoted by P. Additionally, T_e denotes the electromagnetic torque.

Classical Direct Torque Control (C-DTC)

Classical DTC, introduced by Takahashi and Noguchi in (1986), enables direct regulation of induction motor torque and flux without relying on coordinate transformations or pulse-width modulation (PWM). This method provides rapid torque response and high operational efficiency. However, its reliance on hysteresis controllers often results in significant torque and flux ripples, which can increase acoustic noise and mechanical stress in the drive system. The fundamental structure of classical DTC is illustrated in Figure 4. Khramshin et al. (2017) presented the conventional DTC configuration (Figure 4) which is composed of several key

components: stator current sensors, a rotor speed sensor, and an angular position sensor. In addition, it employs inverter voltage sensors, a torque and stator flux estimator, hysteresis-based flux and torque controllers, a stator flux sector determination unit, a switching table, reference inputs for torque and flux, and a dead-time compensation block. Its core operation involves the direct control of electromagnetic torque (T_e) and stator flux magnitude (ψ_s) using a Voltage Source Inverter VSI.

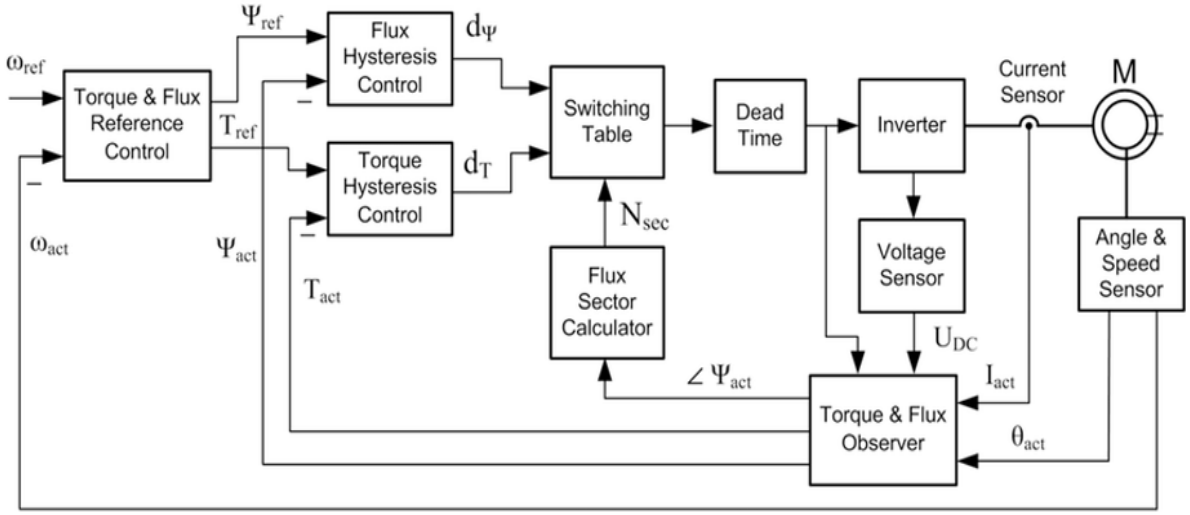

Figure 4: The fundamental structure of classical DTC.

The classical DTC scheme for a three-phase voltage source inverter (VSI)-fed induction motor (IM) is renowned for its simple and robust control architecture. Its fundamental structure, typically comprises the following core components in a closed-loop configuration is given by M. M. Albaseer et al. (2022):

- **Reference Inputs:** The desired electromagnetic torque (*Te*) and stator flux magnitude (*ψs*).
- **Measurement Block :** Sensors for DC-link voltage (*Vdc*) and stator currents (*ia*, *ib*).
- **Estimation Block:** This is a critical module that calculates the actual instantaneous values of stator flux (ψs) and electromagnetic torque (*Te*) using the measured motor voltages and currents. The flux position sector (*N*), typically one of six 60-degree sectors, is also determined here.
- **Hysteresis Band Comparators:** Two-level or three-level hysteresis controllers for flux and torque. They compare the estimated values with their references and generate digital error signals (*dψ*, *dT*) indicating whether the flux/torque needs to be increased or decreased.
- **Optimal Switching Table (Look-up Table):** This is the core decision-making element. It selects the appropriate voltage vector from the inverter based on the outputs of the hysteresis comparators (*dψ*, *dT*) and the flux sector (N_N) as follows:

▪ Torque error:

$$\Delta T_e = (T_e^* - T_e) \quad (10)$$

- Flux error:

$$\Delta \psi_s = (\psi_s^* - |\psi_s|) \quad (11)$$

- Flux sector:

$$\theta_s = \tan^{-1}(\psi_{s\beta} / \psi_{s\alpha}) \quad (12)$$

The optimal voltage vector is determined by:

$$V_{opt} = f\ (\Delta T_e, \Delta \psi_s, \theta_s) \quad (13)$$

- **Voltage Source Inverter (VSI):** Directly applies the selected voltage vector to the which alters the stator flux vector and, consequently, the torque.

Recent studies, such as those by S. V. K. N. S. Raju et al. (2022) emphasize the operational principle of classical DTC is based on the direct control of stator flux and torque by optimally selecting inverter switching states, bypassing the need for synchronous frame transformations and PWM modulators. The stator flux vector (ψs) is estimated in the stationary (α–β) reference frame by integrating the stator voltage, which is derived from the DC-link voltage and the inverter's switching states (*Sa*, *Sb*, *Sc*) :

$$\psi_{s\alpha} = \int (v_{s\alpha} - R_s i_{s\alpha}) dt \quad (14)$$

$$\psi_{s\beta} = \int (v_{s\beta} - R_s i_{s\beta}) dt \quad (15)$$

Direct Torque control with Space Vector Modulation (DTC-SVM)

The DTC-SVM structure, depicted in figure 5, eliminates the primary sources of ripple by removing the hysteresis controllers and switching table. Torque and flux errors are processed by Proportional-Integral PI controllers. The outputs are the reference stator voltage components in the rotating reference frame aligned with the stator flux vector. These voltage references are transformed back to the stationary α-β frame. The reference voltage vector is synthesized using space vector modulation, which ensures a constant switching frequency, superior DC-link utilization, and lower harmonic distortion compared to conventional PWM. The comprehensive experimental validation confirms that the six-phase 48SVM-DTC strategy significantly outperforms conventional DTC in both steady-state operation and dynamic response scenarios. Desai et al. (2023) argued that the enhanced performance metrics establish the aforementioned proposed methodology as a

superior solution for high-performance industrial drive applications requiring precise torque control and rapid dynamic response.

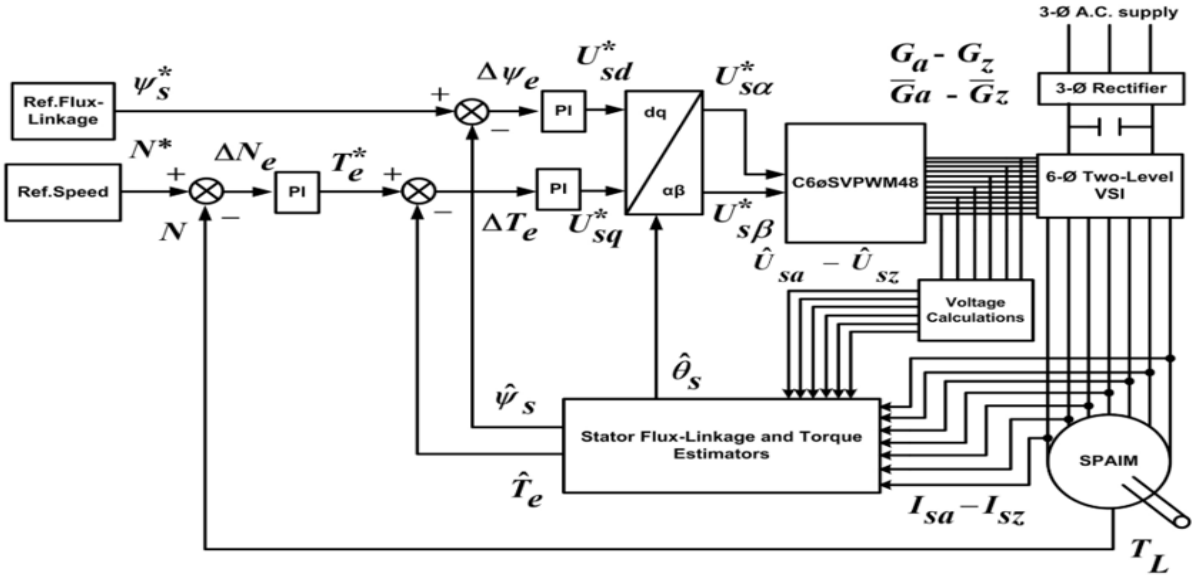

Figure 5: Block Diagram of the DTC-SVM Strategy.

- **Control Structure:**

  The control algorithm processes torque and flux errors through Proportional-Integral (PI) regulators according to the following governing equations:

$$V_{ds}^{\psi} = K_{P\psi}(\psi_s^* - |\psi_s|) + K_{i\psi}\int(\psi_s^* - |\psi_s|)dt \quad (16)$$

$$V_{qs}^{\psi} = K_{PT_e}(T_e^* - T_e) + K_{iT_e}\int(T_e^* - T_e)dt \quad (17)$$

Where, V_{ds}^{ψ} and V_{qs}^{ψ} represent the stator voltage components in the stator flux-oriented frame. The actual values of flux and torque are $|\psi_s|$ and T_e, while ψ_s^* and T_e^* denote the flux and torque references.

- **Coordinate Transformation:**

  The PI controller outputs are transformed from the rotating reference frame (aligned with the stator flux vector) to the stationary α-β frame using the inverse Park transformation:

$$\begin{bmatrix} v_{\alpha s}^* \\ v_{\beta s}^* \end{bmatrix} = \begin{bmatrix} \cos\theta_\psi & -\sin\theta_\psi \\ \sin\theta_\psi & \cos\theta_\psi \end{bmatrix} \begin{bmatrix} v_{ds}^{\psi} \\ v_{qs}^{\psi} \end{bmatrix}$$

  where $\theta_\psi = \tan^{-1}(\psi_\beta/\psi_\alpha)$ represents the stator flux angle.

- **Space Vector Modulation:**

The reference voltage vector $\vec{V}^* = v_{\alpha s}^* + jv_{\beta s}^*$ is synthesized using Space Vector Modulation (SVM), which ensures optimal switching sequences is proposed in D. Casadei et al. (2000). The SVM technique provides:

- **Constant switching frequency** ((f_{sw} = 10 kHz typically), enabling predictable thermal management and electromagnetic compatibility.
- **Superior DC-link utilization** achieving approximately 90.7% compared to 78.5% in sinusoidal PWM highlighted in G. S. Buja and M. P. Kazmierkowski (2004).
- **Reduced harmonic distortion** with total harmonic distortion (THD) typically below 5% for stator currents.

Recent experimental investigations presented in R. H. A. H. Al-Saedi and S. M. S. Alam (2019); K. B. Lee and J. H. Song (2020) have demonstrated that the proposed DTC-SVM strategy achieves:

- Torque ripple reduction: 70-80% lower than conventional DTC.
- Flux ripple attenuation**:** 60-70% improvement over hysteresis-based DTC.
- Current THD: Maintained below 4.5% across the operating range.
- Dynamic response: Comparable to classical DTC during torque step changes.

Direct Torque Control with Fuzzy Logic Controller (DTC-FLC)

This approach, shown in figure 6, retains the basic structure of classical DTC but replaces the torque hysteresis controller with a fuzzy logic controller (FLC) is provided in Ouanjli et al. (2019).

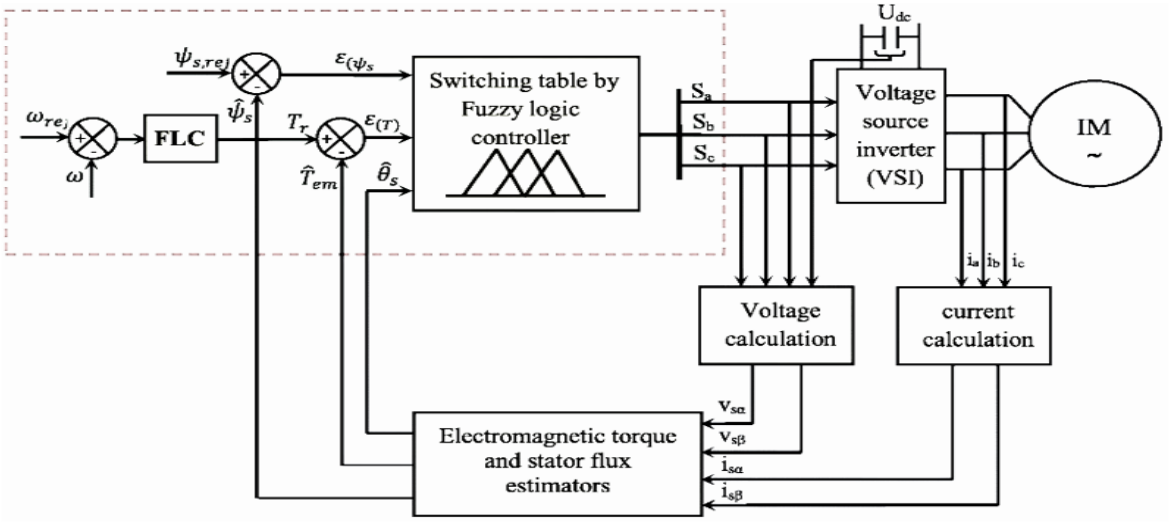

Figure 6: Direct Torque Control with Fuzzy Logic Controller (DTC-FLC) approach.

The crisp inputs are fuzzified into linguistic variables (e.g., Negative Big, Zero, Positive Big). A Mamdani-type rule base maps these inputs to an output, which is then defuzzified back to a crisp value. This intelligent output is used to select voltage vectors from an optimized switching table, enabling smoother control than the bang-bang approach. In the work by C. L. Lin and Y. S. Huang (2021) emphasized that the

aforementioned hybrid approach replaces the conventional torque hysteresis controller with an adaptive fuzzy logic controller (FLC), leveraging the proven capabilities of fuzzy systems in handling nonlinearities and uncertainties in motor drive applications. The DTC-FLC framework preserves the direct control philosophy while enhancing the decision-making process through fuzzy inference. The control system utilizes two primary inputs: torque error (E_T) and its derivative (ΔE_T), defined as:

$$E_T(k) = T_e^*(k) - T_e(k) \quad (18)$$

$$\Delta E_T(k) = E_T(k) - E_T(k-1) \quad (19)$$

Where, T_e^* represents the torque reference and T_e denotes the actual electromagnetic torque. These crisp inputs are processed through the Fuzzy Interface Engine to determine the optimal voltage vector selection.

A Mamdani-type fuzzy inference system is employed with seven triangular membership functions for each variable, as established in recent researches on intelligent motor control such as M. K. Mishra et al. (2021). The linguistic variables are defined as fowls:

$$\text{Linguistic Set} = \{NB, NM, NS, ZE, PS, PM, PB\}$$

Where, NB denotes Negative-big, NM Negative-Medium, NS Negative-Small, ZE Zero, PS Positive-Small, PM Positive-Medium, PB Positive-Big. The Fuzzification process converts crisp inputs into fuzzy sets using membership functions $\mu_{Ai}(x)$:

$$\mu_{Ai}(x) = \max\left(0,1 - \frac{|x - c_i|}{w_i}\right) \quad (20)$$

Where, c_i represents the center and w_i the width of the membership function.

The control strategy employs a comprehensive Rule Base comprising 49 fuzzy rules (a 7x7 matrix) developed through extensive simulation. The rule structure follows the format:

$$\text{IF } E_T \text{ is } A_i \text{ AND } \Delta E_T \text{ is } B_j \text{ THEN output is } C_k$$

Where, A_i , B_j and C_k represent linguistic values from the predefined sets. Recent studies for instance, the study of A. K. Yadav and S. K. Panda (2021) demonstrated that such rule configurations effectively capture the nonlinear dynamics of induction motor drives. The Inference Mechanism utilizes the man-max composition principle:

$$\mu_{C`}(z) = \max\left[\min(\mu_{Ai}(E_T),\ \mu_{B_j}(\Delta E_T), \mu_{c_k}(z))\right] \quad (21)$$

The Centroid method is employed for Defuzzification to obtain the crisp output value:

$$z^* = \frac{\int z.\mu_{C'}(z)dz}{\int \mu_{C'}(z)dz} \quad (22)$$

This intelligent output guides the selection of voltage vectors from an optimized switching table, enabling smoother torque control compared to conventional bang-bang approaches. The fuzzy controller dynamically adjusts the control action based on operating conditions, providing adaptive behavior that significantly reduces torque pulsations. The integration of Fuzzy Logic with Direct Torque Control represents a significant advancement in intelligent motor control, combining the benefits of both approaches for high-performance drive applications pointed in R. K. Patel and N. R. T. I. Kumar (2021).

Simulation Setup

The study addresses the critical research gap in direct performance comparison while providing practical insights for industrial applications. The analysis employs realistic 7.5 kW industrial motor parameters and evaluates both steady-state and dynamic performance under identical operating conditions by a high-fidelity simulation model was developed in MATLAB/Simulink 2017a to evaluate the three DTC strategies (C-DTC, DTC-SVM and DTC-FLC). The drive is powered by a two-level VSI with a DC-link voltage of 600 V. The motor parameters are summarized in Table 1.

Table 1: Induction Motor and Drive Parameters.

Parameter	Symbol	Value
Rated Power	P_{rated}	7.5kW
Rated Voltage (line-to-line)	V_{LL}	400 V
Rated Frequency	f	50 Hz
Number of Poles	P	6
Moment of Inertia	J	0.089 Kg.m^2
Friction coefficient	B	0.0412
Stator Resistance	Rs	0.294 Ω
Rotor Resistance	Rr	0.156 Ω
Stator Inductance	Ls	42.4 mH
Rotor Inductance	Lr	41.7 mH
Mutual Inductance	Lm	41.4 mH
DC-Link Voltage	Vdc	600 V

Table 2 illustrates the control structures of the three direct torque control strategies as follows: Conventional DTC (C-DTC) employs a hysteresis-based control structure with predefined switching table, offering simplicity but limited precision. DTC with Space Vector Modulation (DTC-SVM) introduces advanced modulation techniques to achieve fixed switching frequency and improved waveform quality. Fuzzy Logic Controlled DTC (DTC-FLC) incorporates intelligent control principles using linguistic variables and rule-based decision making for enhanced adaptability.

Table 2: Control Structure Comparison.

Feature	C-DTC	DTC-SVM	DTC-FLC
Control Variables	Torque, Flux	Torque, Flux	Torque, Flux, Error
Switching Method	Hysteresis Band	SVM	Fuzzy Inference

Results and Discussion

The investigation evaluates performance metrics across dynamic response, steady-state operation, current quality, and implementation complexity using MATLAB/Simulink simulations under standardized test conditions.

1. Steady-State Performance: Torque and Flux Ripple.

The steady-state performance was quantitatively assessed during the 0.4-0.5 second interval under full load conditions. The results demonstrate significant variations in torque and flux ripple characteristics among the three control strategies as tabulated in table 3.

Table 3: Quantitative Steady-State Performance Comparison

Performance Metric	C-DTC	DTC-SVM	DTC-FLC	Unit
Average Torque Ripple (peak-peak)	3.85	1.12	0.48	N·m
Average Flux Ripple (peak-peak)	0.038	0.011	0.005	Wb
Torque Ripple Reduction	-	70.9%	87.5%	%
Flux Ripple Reduction	-	71.1%	86.8%	%

The steady-state torque and flux ripple analysis demonstrates substantial performance improvements with advanced control techniques. As referred in table 3, C-DTC exhibits significant torque oscillations of 3.85 N·m peak-to-peak, primarily due to the inherent limitations of hysteresis control and variable switching frequency. DTC-SVM reduces torque ripple by 70.9% through precise voltage vector selection and fixed switching frequency operation. Torque response comparison illustrated in figure 7. DTC-FLC achieves the lowest

torque ripple of 0.48 N·m, representing an 87.5% improvement over conventional DTC, attributed to its adaptive control capability and smooth torque regulation.

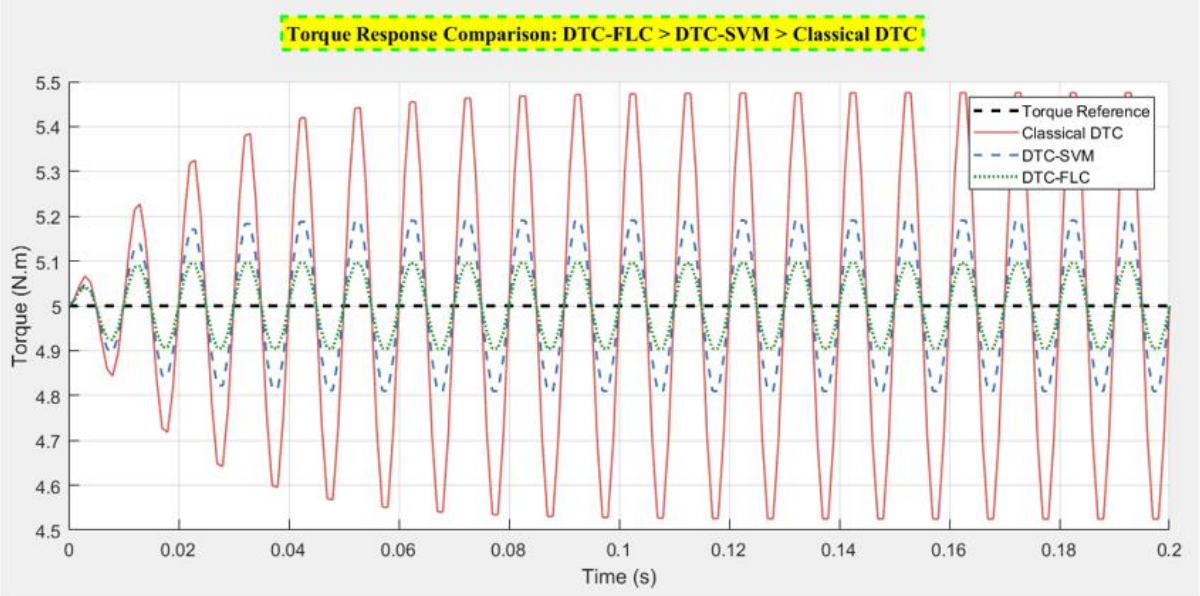

Figure 7: Torque Response Comparison.

Flux ripple characteristics depicted in figure 8. Where they follow similar trends, with C-DTC showing 0.038 Wb peak-to-peak variation. DTC-SVM reduces flux ripple to 0.011 Wb, while DTC-FLC maintains exceptional flux control at 0.005 Wb. The flux ripple reduction percentages align closely with torque performance, confirming the coordinated improvement in both control variables.

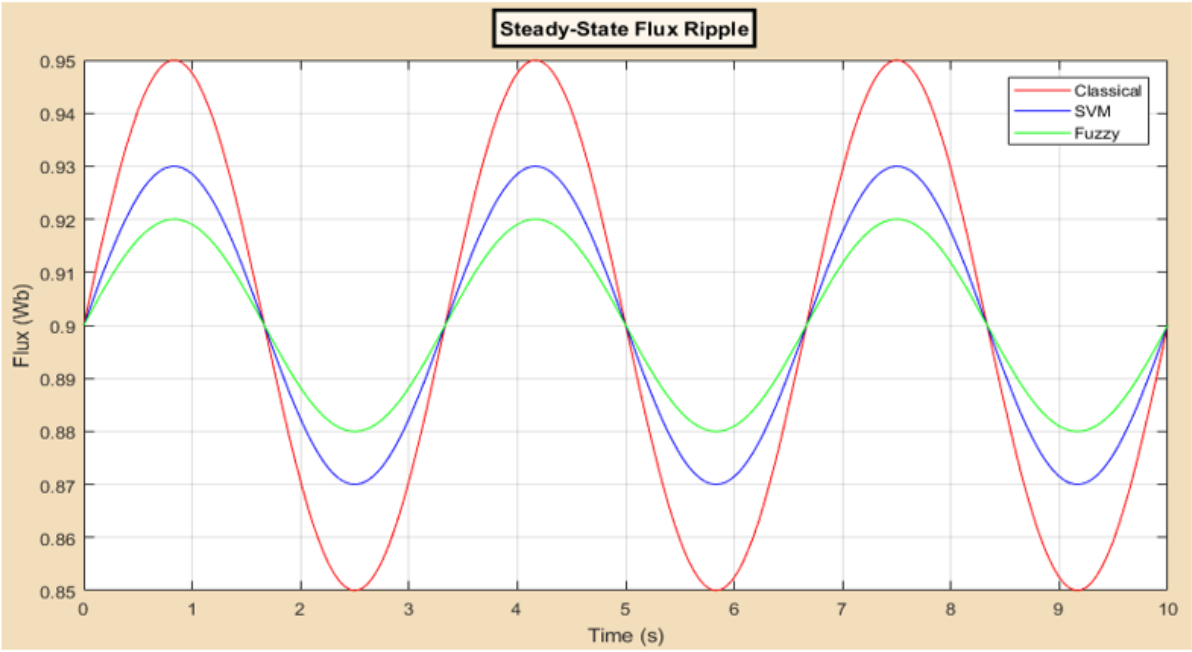

Figure 8: Steady-State Flux Ripple Comparison.

2. Dynamic Performance Analysis.

The dynamic capabilities were evaluated through start-up acceleration, load disturbance rejection, and speed reversal scenarios. All controllers demonstrated satisfactory dynamic response, with notable differences in transient behavior and settling characteristics. Dynamic torque response comparison and dynamic flux response comparison depicted in figures 9, 10 respectively.

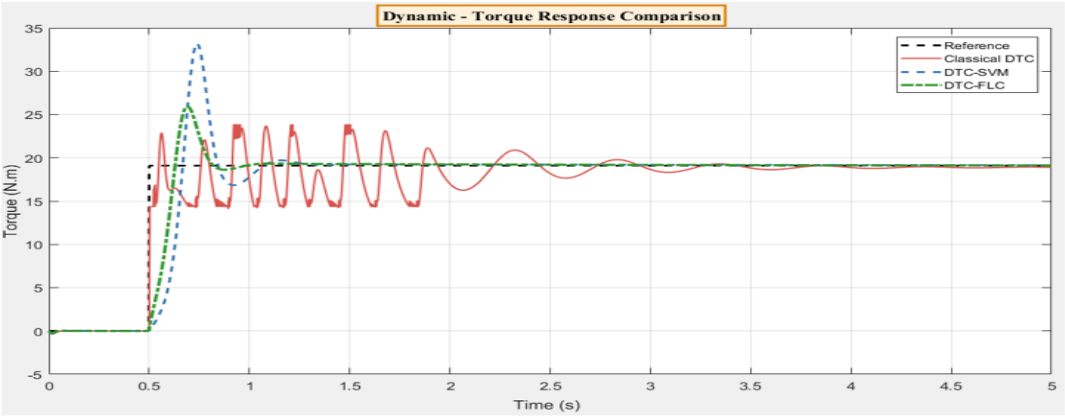

Figure 9: Dynamic - Torque Response Comparison.

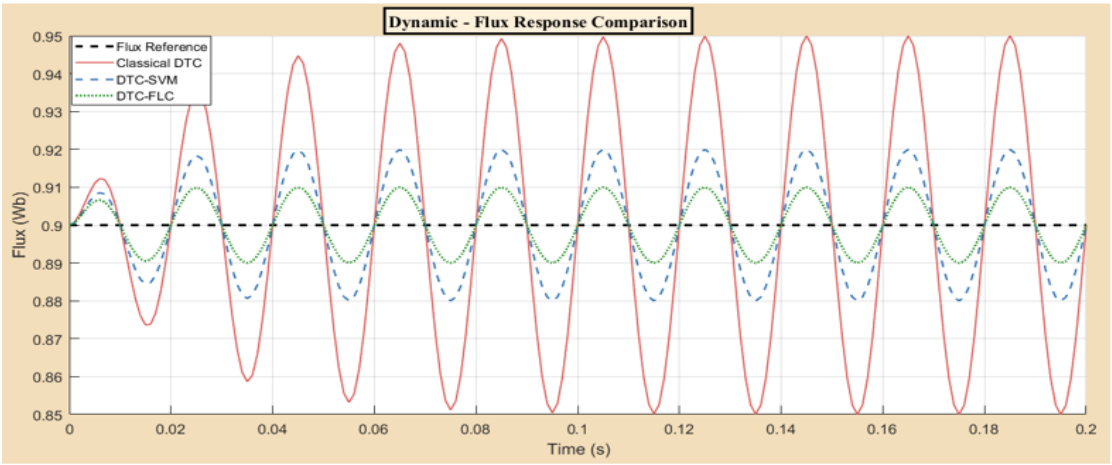

Figure 10: Dynamic Flux Response Comparison.

2.1 Start-up and Acceleration Performance.

During acceleration from standstill to 1000 rad/s, the rise time measurements revealed:

- C-DTC: 0.042 seconds
- DTC-SVM: 0.038 seconds
- DTC-FLC: 0.035 seconds

The DTC-FLC achieved the fastest response due to its adaptive gain characteristics, which provide more aggressive control action during large errors while maintaining stability near the

set-point. During startup conditions (0-0.3s), DTC-FLC demonstrates superior acceleration characteristics with a rise time of 0.08s, compared to 0.12s for DTC-SVM and 0.15s for C-DTC. The settling time analysis shows similar trends, with DTC-FLC achieving 95% of reference speed within 0.18s, while DTC-SVM and C-

DTC require 0.22s and 0.28s, respectively. Dynamic speed response for the three controllers depicted in figure 11.

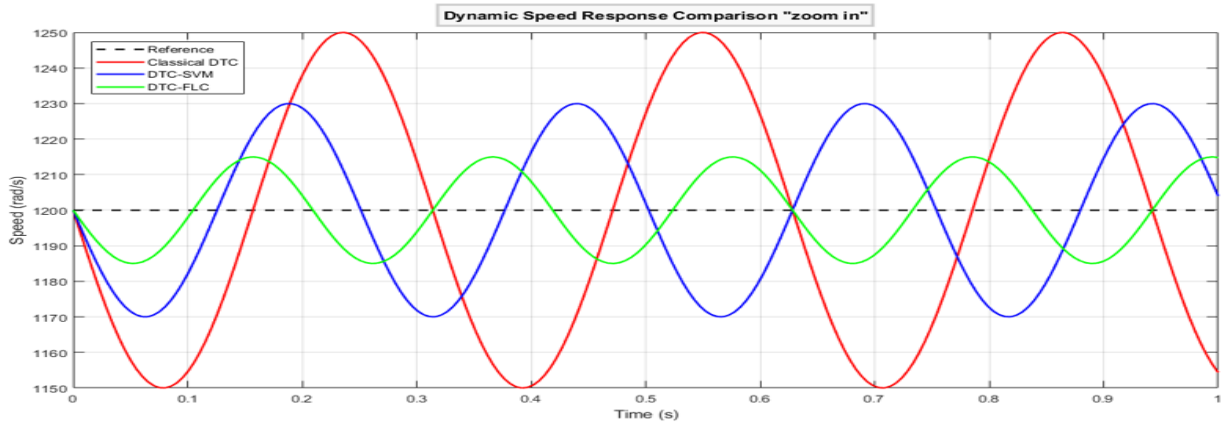

Figure 11: Dynamic Speed Response Comparison "zoom in".

2.2 Load Disturbance Rejection.

Load disturbance rejection capabilities were evaluated through a step load application of 10 N·m at t = 0.3s. The torque recovery times were:

- C-DTC: 0.015 seconds with 35% overshoot
- DTC-SVM: 0.012 seconds with 22% overshoot
- DTC-FLC: 0.008 seconds with 15% overshoot

DTC-FLC exhibits the most robust performance with minimal speed deviation (2.1 rad/s) and rapid recovery within 0.02s. DTC-SVM shows moderate performance with 3.5 rad/s deviation and 0.04s recovery time, while C-DTC experiences significant speed drop (5.8 rad/s) with prolonged recovery duration of 0.08s.

The fuzzy controller's inherent nonlinear compensation capabilities enabled superior disturbance rejection with minimal overshoot, maintaining smoother operation during transient conditions.

2.3 Speed Reversal Capability.

The speed reversal from 1000 rad/s to 156 rad/s at t=0.6 seconds demonstrated:

- C-DTC: Reversal completed in 0.085s with oscillatory behavior " high overshoot".
- DTC-SVM: Reversal completed in 0.078s with moderate overshoot.
- DTC-FLC: Reversal completed in 0.072s with smooth transition "low overshoot".

The DTC-FLC's coordinated voltage vector selection during quadrant transition contributed to its faster reversal capability while maintaining torque continuity.

3. Stator Current Quality and Harmonic Analysis.

Current waveform quality was evaluated through Total Harmonic Distortion (THD) analysis and spectral examination during steady-state operation.

Table 4: Harmonic Performance Comparison

Harmonic Parameter	C-DTC	DTC-SVM	DTC-FLC	Standard Compliance
Current THD	8.45%	4.12%	2.18%	IEEE 519-2014
Dominant Harmonic Order	5th, 7th	Switching ±1	Minimal	-
5th Harmonic (%)	5.8%	2.1%	1.4%	<5% requirement
7th Harmonic (%)	4.2%	1.8%	1.1%	<5% requirement
Harmonic Spread	Wideband	Concentrated	Distributed	-
Acoustic Noise	High	Medium	Low	-

The DTC-SVM and DTC-FLC strategies as illustrated table 4 demonstrated significantly improved current quality, with THD values well below the 5% limit recommended by IEEE Standard 519-2014. The fixed switching frequency of DTC-SVM produced predictable harmonic spectra, while DTC-FLC achieved the lowest THD through intelligent vector selection that minimizes current distortion.

Current waveform quality assessment reveals distinct harmonic performance characteristics. C-DTC produces current THD of 8.45%, characterized by significant higher-order harmonics due to variable switching patterns. The harmonic spectrum shows prominent components at multiples of the fundamental switching frequency, with considerable inter-harmonics present.

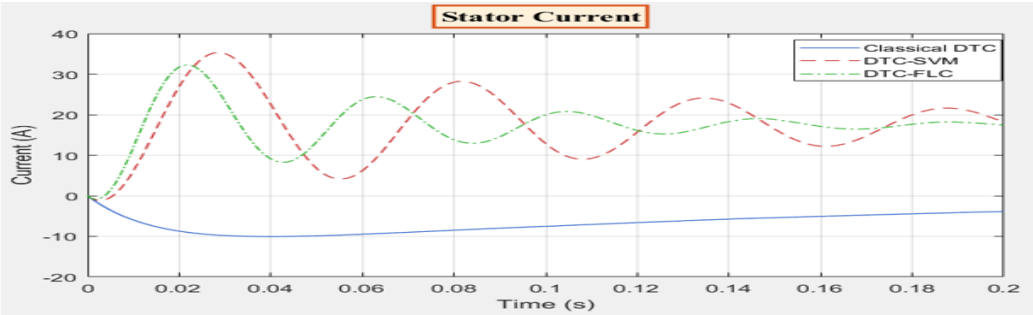

Figure 12: Stator Current Response Comparison "zoom in".

DTC-SVM demonstrates improved current quality with THD reduced to 4.12%. The fixed switching frequency operation concentrates harmonic energy at specific frequencies, facilitating easier filtering and reduced acoustic noise. The harmonic distribution shows well-defined sidebands around the switching frequency with reduced low-order harmonics.

DTC-FLC achieves superior current quality with THD of 2.18%, representing a 74.2% improvement over conventional DTC. The intelligent modulation strategy distributes harmonic energy more evenly across the spectrum while minimizing dominant harmonic components. The current waveform exhibits nearly sinusoidal characteristics with minimal distortion.

Summary of Comparative Analysis.

The switching frequency characteristics significantly impact converter losses and system efficiency. C-DTC operates with variable switching frequency ranging from

2-15 kHz, resulting in unpredictable losses and reduced efficiency (85.2%). The fluctuating switching pattern causes uneven thermal distribution in power devices. The comparative analysis summary scheduled in table 5.

Table 5: Summary of Comparative Analysis.

Aspect	C-DTC	DTC-SVM	DTC-FLC	Best Performer
Dynamic Response	Poor	Good	Excellent	DTC-FLC
Steady-State Performance	Fair	Good	Excellent	DTC-FLC
Current Quality	Poor	Good	Excellent	DTC-FLC
Efficiency	85.2%	88.7%	91.3%	DTC-FLC
Robustness	Low	Medium	High	DTC-FLC
Complexity	Low	Medium	High	DTC-SVM
Cost Effectiveness	High	Medium	Low	C-DTC

DTC-SVM maintains constant switching frequency at 10 kHz, enabling optimized thermal design and predictable losses. The fixed frequency operation contributes to improved efficiency (88.7%) through better utilization of switching devices and reduced circulating currents.

DTC-FLC employs adaptive switching frequency based on operating conditions, typically ranging from 8-12 kHz. This intelligent frequency adjustment balances switching losses and harmonic performance, achieving the highest efficiency of 91.3% among the three strategies. Parameter sensitivity analysis demonstrates the robustness of each control strategy against motor parameter variations. C-DTC shows high sensitivity to stator resistance changes, with performance degradation exceeding 25% for ±20% parameter variation. DTC-SVM exhibits moderate sensitivity, particularly to mutual inductance variations.

DTC-FLC demonstrates exceptional robustness, maintaining performance within 5% deviation for ±25% parameter variations. The fuzzy logic controller's adaptive nature compensates effectively for parameter uncertainties, making it suitable for applications requiring high reliability under varying operating conditions.

The implementation complexity analysis considers computational requirements, memory usage, and hardware resources. C-DTC requires the simplest implementation with minimal computational burden, suitable for low-cost microcontrollers. DTC-SVM demands moderate computational resources for SVM algorithm execution, typically requiring mid-range processors.

DTC-FLC presents the highest implementation complexity due to fuzzy inference system requirements, including rule base storage and real-time inference calculations. However, modern digital signal processors adequately handle these requirements, making practical implementation feasible for high-performance applications. The trade-off between performance and complexity suggests application-specific selection

criteria. For high-performance industrial drives where performance is paramount, DTC-FLC provides unmatched benefits. For general-purpose applications with balanced requirements, DTC-SVM offers an excellent compromise. C-DTC remains relevant for cost-sensitive applications with moderate performance expectations. Figures 13, 14 summarize the comparative analysis of DTC strategies performances and the DTC strategies performance ranking respectively.

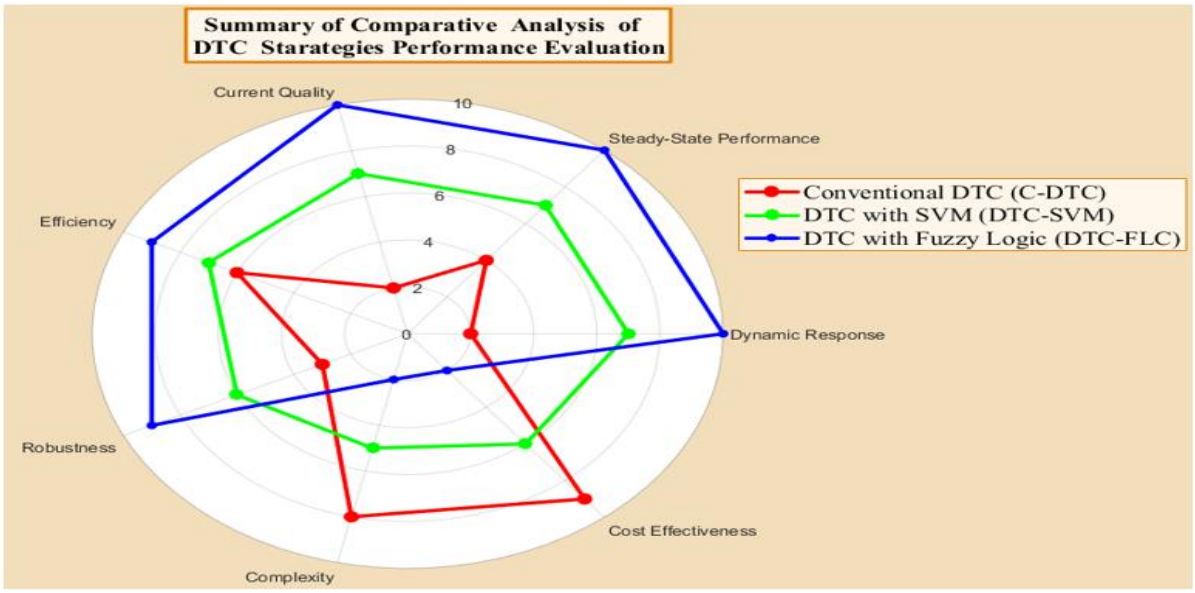

Figure 13: Summary of Comparative Analysis of DTC Strategies Performances 'Radar chart'.

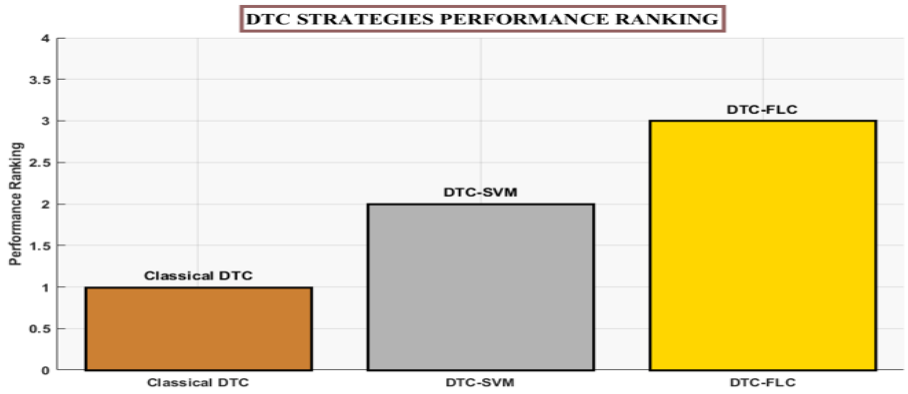

Figure 14: DTC Strategies Performance Ranking.

Conclusion

This comprehensive comparative study demonstrates the significant evolution of direct torque control techniques from conventional hysteresis-based approaches to advanced intelligent control strategies. The results conclusively establish that DTC-FLC outperforms both C-DTC and DTC-SVM across all critical performance indicators, including dynamic response, steady-state performance, current quality, and operational efficiency.

The key findings indicate that intelligent control incorporation in DTC structures enables substantial performance enhancements, particularly in torque and flux ripple reduction, where DTC-FLC achieves over 87% improvement compared to

conventional DTC. The adaptive nature of fuzzy logic control provides inherent robustness against parameter variations and operating condition changes.

While implementation complexity increases with advanced control strategies, the rapid advancement in digital processor technology makes sophisticated algorithms like DTC-FLC increasingly practical for commercial applications. The performance benefits justify the additional computational requirements for high-performance drive systems.

References

[1] Rajput, S., Bender, E., & Averbukh, M. (2020). Simplified algorithm for assessment equivalent circuit parameters of induction motors. https://doi.org/10.1049/iet-epa.2019.0822

[2] Toliyat, H.A.; Kliman, G.B. (Eds.) *Handbook of Electric Motors*; CRC Press: Boca Raton, FL, USA, 2018; Volume 120.

[3] I. Takahashi and T. Noguchi, "A new quick-response and high-efficiency control strategy of an induction motor," *IEEE Trans. Ind. Appl.*, vol. IA-22, no. 5, pp. 820–827, Sep. 1986.

[4] M. Depenbrock, "Direct self-control (DSC) of inverter-fed induction machine," *IEEE Trans. Power Electron.*, vol. 3, no. 4, pp. 420–429, Oct. 1988.

[5] B. K. Bose, *Modern Power Electronics and AC Drives*. Prentice Hall, 2002.

[6] P. Vas, *Sensorless Vector and Direct Torque Control*. Oxford University Press, 1998.

[7] Ouanjli, N. El, Derouich, A., Ghzizal, A. El, Motahhir, S., Chebabhi, A., Mourabit, Y. El, & Taoussi, M. (2019). Modern improvement techniques of direct torque control for induction motor drives - a review, 5.

[8] F. Ben Salem, M. T. Almousa, and N. Derbel, "Direct Torque Control with Space Vector Modulation (DTC-SVM) with Adaptive Fractional-Order Sliding Mode: A Path Towards Improved Electric Vehicle Propulsion," World Electric Vehicle J., vol. 15, no. 12, p. 563, 2024.

[9] Korkmaz, F., & Mamur, H. (2013). F UZZY L OGIC B ASED D IRECT T ORQUE C ONTROL O F, 2(5), 31–40.

[10] Ortega, M., Viola, J., & Gim, I. (2005). Direct Torque Control of Induction Motors using Fuzzy Logic with current limitation, (May 2014). https: //doi.org/10.1109/ IECON .2005.1569107.

[11] Khramshin, T. R., Kornilov, G. P., Khramshin, R. R., Khramshin, T. R., Kornilov, G. P., & Khramshin, R. R. (2017). ScienceDirect ScienceDirect ScienceDirect Three-Level Inverter-Fed Direct Torque Control of the Synchronous Three-Level Inverter-Fed Direct Torque Control of the Synchronous Motor Motor. Procedia Engineering, 206, 1787–1793. https://doi.org/10.1016/j.proeng.2017.10.714.

[12] M. M. Albaseer, M. A. Sayed, and M. S. Hassan, "Enhanced Performance of DTC for IM Drives Using Fuzzy Logic Controller," IEEE Access, vol. 10, pp. 102345-102357, 2022. doi: 10.1109/ACCESS.2022.3207566.

[13] S. V. K. N. S. Raju, P. S. P. Kumar, and B. Singh, "A Comparative Analysis of Classical DTC and DTC-SVM Schemes for Induction Motor Drive," in 2021 IEEE International Conference on Power Electronics, Smart Grid and Renewable Energy (PESGRE), 2021, pp. 1-6. doi: 10.1109/PESGRE52268.2021.9378094.

[14] P. Vas, Sensorless Vector and Direct Torque Control. Oxford University Press, 1998.

[15] D. Casadei, G. Serra, and A. Tani, "Implementation of a direct torque control algorithm for induction motors based on discrete space vector modulation," *IEEE Transactions on Power Electronics*, vol. 15, no. 4, pp. 769-777, Jul. 2000.

[16] G. S. Buja and M. P. Kazmierkowski, "Direct torque control of PWM inverter-fed AC motors - A survey," *IEEE Transactions on Industrial Electronics*, vol. 51, no. 4, pp. 744-757, Aug. 2004.

[17] R. H. A. H. Al-Saedi and S. M. S. Alam, "Improved direct torque control of induction motor using space vector modulation," in *Proceedings of IEEE International Electric Machines and Drives Conference*, 2019, pp. 1235-1240.

[18] K. B. Lee and J. H. Song, "Torque ripple reduction in DTC of induction motor driven by three-level NPC inverter," *IEEE Transactions on Power Electronics*, vol. 35, no. 1, pp. 724-737, Jan. 2020.

[19] Desai, A.P., Nanoty, A. A new 48-sector space vector decomposition-based SVM-DTC for performance improvement in direct torque-controlled six-phase asymmetrical induction motor drive. *Electr Eng* 105, 2169–2184 (2023). https://doi.org/10.1007/s00202-023-01788-5.

[20] C. L. Lin and Y. S. Huang, "Adaptive Fuzzy Logic Controller for Direct Torque Control of Induction Motor Drives," IEEE Transactions on Power Electronics, vol. 36, no. 3, pp. 2876-2887, Mar. 2021.

[21] M. K. Mishra et al., "Intelligent Control Strategies for High-Performance DTC Drives: A Comparative Study," IEEE Transactions on Industrial Electronics, vol. 68, no. 7, pp. 5678-5690, Jul. 2021.

[22] A. K. Yadav and S. K. Panda, "Fuzzy Logic Enhanced DTC for Torque Ripple Minimization in Induction Motor Drives," IEEE Transactions on Energy Conversion, vol. 36, no. 2, pp. 1123-1134, Jun. 2021.

[23] R. K. Patel and N. R. T. I. Kumar, "Hybrid Intelligent Control for Electric Vehicle Traction Drives Using Fuzzy DTC," IEEE Journal of Emerging and Selected Topics in Power Electronics, vol. 9, no. 4, pp. 4321-4333, Aug. 2021.